NeuroImage: Clinical 24 (2019) 102096

Contents lists available at ScienceDirect

NeuroImage: Clinical

journal homepage: www.elsevier.com/locate/ynicl

Blue light activates pulvinar nuclei in longstanding idiopathic photophobia: A case report

Athanasios Panorgias[a], Danielle Lee[b], Katie E. Silva[b], David Borsook[b,c], Eric A. Moulton[b,c,d,*,1]

[a] Department of Vision Science, New England College of Optometry, Boston, MA, USA
[b] Center for Pain and the Brain, Boston Children's Hospital, Massachusetts General Hospital, McLean Hospital, Boston, MA, USA
[c] Department of Anesthesiology, Perioperative and Pain Medicine, Boston Children's Hospital, Harvard Medical School, Boston, MA, USA
[d] Department of Ophthalmology, Boston Children's Hospital, Harvard Medical School, Boston, MA, USA

ARTICLE INFO

Keywords:
Melanopsin
Photo-oculodynia
Photalgia
Photoallodynia
Pain
ipRGCs

ABSTRACT

Numerous pathologies can contribute to photophobia. When considering light transduction alone, photophobia may be triggered through melanopsin pathways (non-image forming), rod and cone pathways (image-forming), or some combination of the two. We evaluated a 39 year old female patient with longstanding idiopathic photophobia that was exacerbated by blue light, and tested her by presenting visual stimuli in an event-related fMRI experiment. Analysis showed significantly greater activation in bilateral pulvinar nuclei, associated with the melanopsin intrinsically photosensitive retinal ganglion cell (ipRGC) visual pathway, and their activation is consistent with the patient's report that blue light differentially evoked photophobia. This appears to be the first demonstration of functional activation of the ipRGC pathway during photophobia in a patient.

1. Introduction

Photophobia is a common and debilitating symptom that describes painful sensitivity to light. It is often associated with migraine and other neurological disorders, but can also arise from ocular pathologies, psychiatric conditions, and as a pharmacological side effect (Albilali and Dilli, 2018; Katz and Digre, 2016; Noseda et al., 2018). Despite its common prevalence, photophobia remains poorly understood. This is perhaps due to the wide variety of pathologies that can cause this symptom.

Even when considering only light transduction in the eye, photophobia may be triggered through melanopsin pathways (non-image forming), rod and cone pathways (image-forming), or through some combination of the two. At least three melanopsin pathways have been proposed for primates and non-primate mammals: (1) in the retina, intrinsic photosensitive retinal ganglion cells (ipRGCs) containing melanopsin photopigment activate nociceptive trigeminovascular thalamic neurons (Noseda et al., 2010); (2) in the iris (Xue et al., 2011), melanopsin-containing nociceptive-afferents are activated by light (Dolgonos et al., 2011); and (3) in the cornea, melanopsin is expressed on and directly activates trigeminovascular afferents (Matynia et al., 2016), which may be sensitized by ocular surface injury (Moulton et al., 2009). With traditional retinal light transduction pathways, photophobia has been proposed to act through (1) rods and cones parasympathetically triggering ocular vasodilation, which in turn activate trigeminal nociceptive afferents in blood vessels, (Okamoto et al., 2010) or (2) cone pathways relaying light signals to nociceptive trigeminovascular thalamic neurons (Noseda et al., 2010). The common theme is the intersection of afferent visual processing with nociceptive trigeminal pathways (Katz and Digre, 2016; Noseda et al., 2018; Rosenthal and Borsook, 2012).

We evaluated a patient who suffered from longstanding idiopathic photophobia with no diagnosis of migraine. The patient reported that her longstanding painful sensitivity to light was markedly reduced when she wore FL-41 tinted lenses (TheraSpecs Co., Phoenix, AZ). The FL-41 tint maximally filters wavelengths of light within the spectral sensitivity of melanopsin, around 480 nm. This case study provided an opportunity to identify the neural circuitry underlying photophobia that is presumably mediated by melanopsin.

We hypothesized that with the presentation of blue light to this patient, we would evoke photophobia and see functional magnetic resonance imaging (fMRI) activation of nociceptive trigeminal pathways.

1.1. Case report

A 39-year-old Caucasian female presented with longstanding

* Corresponding author: Eric Moulton OD, PhD, Center for Pain and the Brain, Boston Children's Hospital, 1 Autumn Street, Boston, MA 02215.
E-mail address: eric.moulton@childrens.harvard.edu (E.A. Moulton).
[1] www.childrenshospital.org

https://doi.org/10.1016/j.nicl.2019.102096
Received 8 April 2019; Received in revised form 10 November 2019; Accepted 15 November 2019
Available online 16 November 2019

idiopathic photophobia. She reported that exposure to blue light produced constant eye pain and that her vision would become blurry, as if there were "like talcum powder sprinkled in the air." She also reported contraction of muscles in her face, nausea, increased heart rate, strong negative affect, and a "strong sense of fear and isolation." She indicated that she has had these symptoms for as long as she can remember, and did not report any similar history of photophobia in family members.

The subject had managed her photophobia using Theraspecs FL-41 tinted lenses for the past three years. She reported that when she first wore these lenses, her lifelong anxiety related to photophobia "decreased dramatically within 2 days." She noted that the therapeutic effect was instantaneous when she wore them. She reported no major sleep/wake cycle issues, though she occasionally took sedatives as a sleep aid.

Her medical history was positive for myofascial pain syndrome, fibromyalgia, Asperger's Syndrome, congenital heart defects, and polycystic ovarian syndrome. Aside from photophobia, she reported no symptoms consistent with migraine, and had not been diagnosed with migraine. She had previously received a CT scan and a 17-channel EEG (Baton Rouge Clinic 2012), both diagnosed as normal. For medications, she reported taking Niacin (500 mg), and low-dose Naltrexone (4.5 mg) for her fibromyalgia.

Her previous eye exams (in 2012, 2014, and 2016) revealed no pathology of the cornea or retina, despite photophobia being reported as the chief complaint. These exams were each performed by independent ophthalmologists. Optical coherence tomography (OCT, 2014) were reported as normal and revealed no ocular pathology or signs of retinal dystrophy. Her electroretinogram records (ERG, 2014) indicated normal inner and outer retinal responses (a- and b-wave amplitudes, latency, and shape) under dark-adapted rod-only conditions, normal responses in dark-adapted bright flash test conditions, normal responses in light-adapted conditions, and normal amplitudes and latencies with 30 Hz flicker testing. Fluorescein angiography (2012) showed normal vascular fill time with no leakage or ischemia.

2. Methods

This study was approved by the McLean Hospital Institutional Review Board, and met the scientific and ethical guidelines for human research of the Helsinki Accord (http://ohsr.od.nih.gov/guidelines/helsinki.html). The subject provided written informed consent to participate in this study.

The subject participated in a 1-hour session during which she was presented with visual stimuli in an event-related fMRI experiment. During fMRI scanning, the subject used a prism mirror to view a presentation projected on a screen just outside of the scanner bore. The stimuli were presented on a screen subtending 17 × 12° of visual angle by a Cannon WUX 500 projector. The stimuli were presented bilaterally, as the patient viewed them binocularly.

2.1. Stimulation protocol

The protocol consisted of a bilateral stimulus that triggered the patient's symptoms (SYMPT), a stimulus that did not elicit any symptoms (ASYMPT), and a baseline that featured a black screen with a fixation cross. The SYMPT and ASYMPT stimuli were checkerboards with squares that each subtended 0.5° of visual angle, reversing at 7 Hz. The SYMPT stimulus consisted of white and blue checks with ~80% luminance contrast, of which the blue checks were generated using only the blue LED of the projector. The ASYMPT stimulus consisted of white and red checks with ~80% luminance contrast, of which the red checks were generated using only the red LED of the projector. The difference in melanopsin activation between the SYMPT and ASYMPT conditions was ~78%, with the SYMPT condition eliciting the greater melanopsin response. The subject stayed awake and attentive throughout the scan, confirmed by close observation and also quantitatively by noting no motion artifacts in the fMRI data that normally accompany changes in consciousness.

Each checkerboard stimulus was presented in 6-second blocks, with nine SYMPT and nine ASYMPT blocks presented in pseudorandom order. To avoid anticipatory processes, the inter-stimulus interval (ISI) was varied between 51 s and 66 s in 3-second increments, to match the fMRI acquisition. The total duration of the fMRI stimulus paradigm was 19 min 30 s. The scanner environment was kept dark during the entire experiment, with only the projector providing intermittent brief illumination. At the end of the session, the subject retrospectively rated light-evoked pain intensity and unpleasantness on a numerical rating scale (0–10). The extremes of the pain intensity scale were marked "None" and "Most intense pain imaginable", and the extremes for the unpleasantness scale were marked "None" and "Most unpleasant imaginable."

2.2. fMRI imaging

Imaging was conducted using a 3T Siemens Trio scanner (Erlangen, Germany) with a phased-array head coil. For anatomical scans, a sagittal three-dimensional T1-weighted scan (MPRAGE) was performed (TE/TR = 2.74/2100 msec; field of view = 256 mm^2; slice thickness = contiguous 1.33 mm; in-plane resolution = 1.00 mm). For the functional scan, a gradient echo (GE) echo planar imaging (EPI) sequence was performed (TE/TR = 30/2000 ms; field of view = 264 mm^2; slice thickness = contiguous 1.50 mm; in-plane resolution = 1.94 mm), with 585 vol (19 min 30 s) captured. The functional scan consisted of 84 slices oriented in an oblique plane, to match the brainstem axis. This orientation of acquisition has proven useful for functional imaging of brainstem structures (Moulton et al., 2009).

2.3. Data analysis

Functional imaging datasets were processed and analyzed using FEAT (FMRI Expert Analysis Tool) Version 6.00, part of FSL 5.0.0 (FMRIB's Software Library, www.fmrib.ox.ac.uk/fsl) (Smith et al., 2004). Pre-processing included elimination of the first four acquired volumes to allow for signal equilibration; motion correction using MCFLIRT (Motion Correction using FMRIB's Linear Image Registration Tool) (Jenkinson et al., 2002); removal of non-brain structures using BET [Brain Extraction Tool] (Smith, 2002); spatial smoothing using a Gaussian kernel of 5-mm full-width half-maximum; grand-mean intensity normalization of the entire 4D dataset by a single multiplicative factor; and high-pass temporal filtering (Gaussian-weighted least-squares straight line fitting with sigma = 50.0 s). Fixed effects time-series analysis using the general linear model was implemented with FILM (FMRIB's Improved Linear Model) with local autocorrelation correction (Woolrich et al., 2001). The hemodynamic response was modeled using a gamma convolution (SD = 3 s; mean lag = 6 s) of the checkerboard stimulation block, which included three volumes during the stimulus. Each activation map (SYMPT and ASYMPT) thus reflects a comparison of nine stimulus events (totaling 27 vol) vs. 527 vol of baseline. A contrast was included between the SYMPT (blue photophobic state) and ASYMPT (red non-photophobic state) explanatory variables. The statistical parametric maps for each session and contrast maps were co-registered to the high-resolution anatomical scan using FLIRT (FMRIB's Linear Image Registration Tool) (Jenkinson and Smith, 2001). Registration to Montreal Neurological Institute (MNI) standard space was achieved using Advanced Normalization Tools 2.3.1 (Avants et al., 2011). Z-statistic images were thresholded using clusters determined by $Z > 3.1$ and a (corrected) cluster significance threshold of $P = 0.05$ (Worsley, 2001).

3. Results

The subject rated the SYMPT blue stimulus as 2/10 for pain

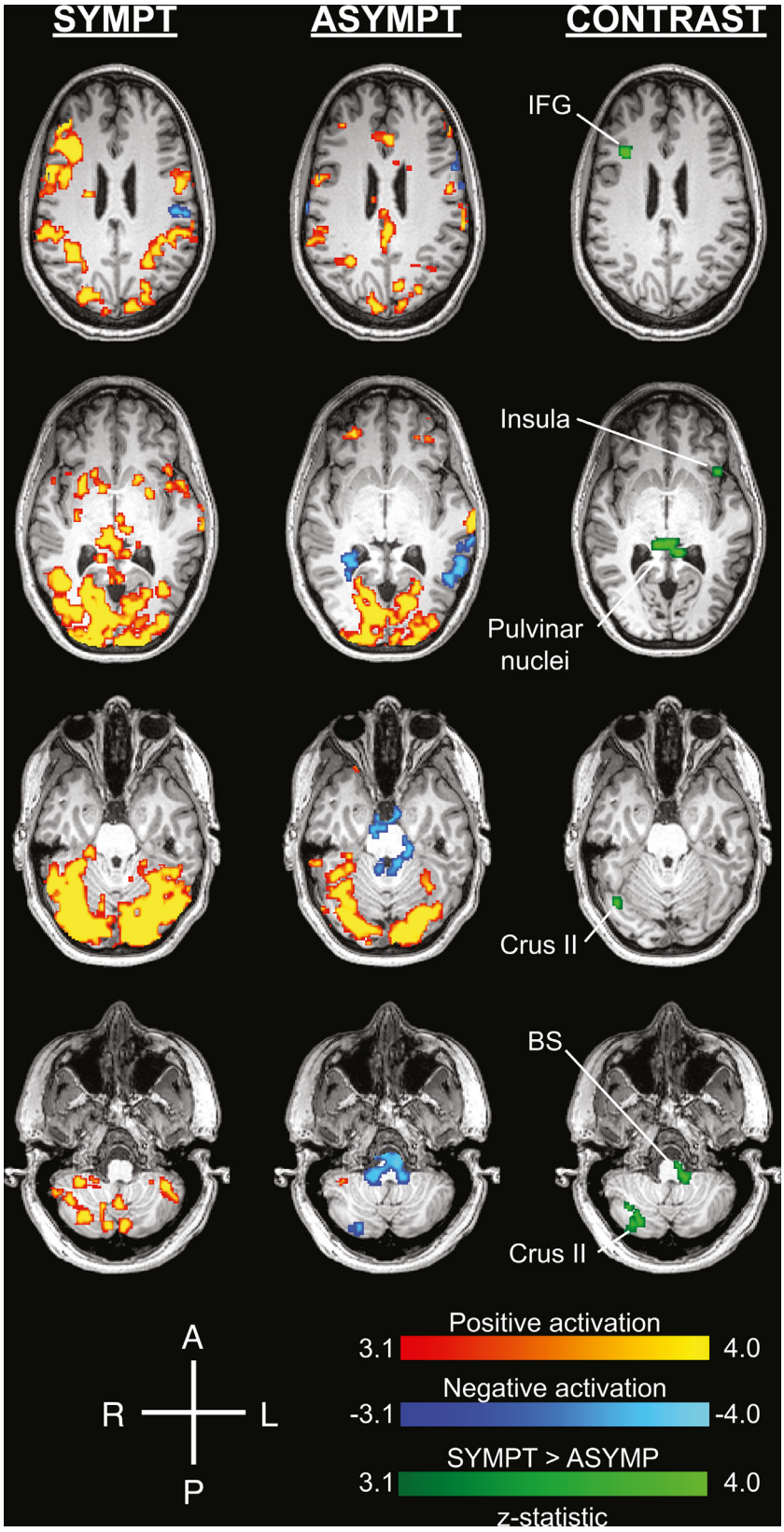

Fig. 1. Pulvinar nuclei, anterior insula, cerebellar crus II, and inferior frontal gyrus are significantly more activated with the photophobia-evoking stimulus (SYMPT) than the control (ASYMPT). Visual cortex and other brain areas were significantly activated in response to the SYMPT condition and the ASYMPT condition. The green represents areas that showed a significant contrast in SYMPT > ASYMPT. No regions were found where a significant contrast was found in ASYMPT > SYMPT. The images are displayed in the patient's native high-resolution space to avoid potential artifacts from spatial transformation to a standard brain atlas. Significant activations and contrasts were thresholded using clusters determined by $Z > 3.1$ and a (corrected) cluster significance threshold of $P = 0.05$. A = anterior, BS = brainstem, IFG = inferior frontal gyrus, L = left, P = posterior, R = right.

intensity and 6/10 for unpleasantness; she rated the ASYMPT red stimulus as 0/10 for pain intensity and 0/10 for unpleasantness. She reported that the SYMPT stimulus onset immediately produced a painful, unpleasant sensation and general feeling of malaise, which would cease the moment the stimulus ended.

Both SYMPT and ASYMPT conditions produced robust cortical activation, particularly in visual cortices (Fig. 1, Table 1, Table 2). Activation in bilateral pulvinar nuclei was significantly greater with SYMPT than ASYMPT stimulation (Fig. 1, Table 3). Other areas with significantly greater activation under SYMPT conditions included right

Table 1
SYMPT Activation.

Brain Region	Side	MNI*	Max Z-stat
Intracalcarine	B	−9, −87, −1	9.62
Middle Frontal Gyrus	R	40,25,20	8.64
Paracingulate Gyrus	R	4,9,52	7.08
	B	0,24,42	5.23
Thalamus (Pulvinar)	R	10, −29, −1	6.19
Lateral Occipital	L	−35, −61,58	6.13
Cerebellum VIIb	L	−6, −76, −44	6.12
	R	31, −69, −52	5.42
Thalamus	R	13, −3,14	6.07
	L	−12, −20, −1	4.44
	L	−25, −32, −1	4.03
	L	−4, −13, −2	3.98
Cerebellar Crus II	L	−39, −43, −44	5.91
Cerebellum VIIIa	R	32, −42, −47	5.55
Supramarginal Gyrus	R	60, −23,36	5.06
Frontal Pole	R	36,39,39	5.4
	L	−32,47,35	4.86
	R	8,62,34	4.41
Precentral Gyrus	L	−59,3,13	5.27
	R	41, −11,46	5.01
Cerebellar Vermis IX	B	0, −53, −37	5.18
Putamen	R	29,10, −5	4.89
	L	−22,4,4	4.83
	R	31,0,5	4.18
Caudate	L	−12,4,20	4.80
	R	11,8,4	4.28
	L	−17, −16,20	3.79
Inferior Frontal Gyrus	R	56,20,6	4.72
	R	43,33,5	4.23
Occipital Pole	B	2, −100, −9	4.56
	R	9, −88,36	4.04
Postcentral Gyrus	L	−66, −21,25	4.36
	R	54, −17,25	4.23
Parahippocampal Gyrus	R	23, −30, −22	4.41
Frontal Operculum	R	37,12,12	4.21
Insula	L	−44,12, −5	4.13
	R	33, −14,15	3.91
Superior Parietal Lobule	R	28, −49,40	3.94
Cuneal	B	0, −78,29	3.84

* MNI = Montreal Neurological Institute standard space.

Table 2
ASYMPT Activation.

Brain Region	Side	MNI*	Max Z-stat
Lingual	B	−1, −81, −2	10.2
Frontal Orbital	R	33,29, −27	6.16
	R	23,6, −19	4.69
Precuneous	R	16, −36,46	5.71
	L	−12, −65,39	4.71
Superior Temporal Gyrus	L	−66, −14,1	5.68
Cerebellum Vermis IX	B	0, −55, −36	5.67
Precentral Gyrus	L	−42, −3,38	5.65
Planum Polare	L	−41, −11, −15	5.30
Supramarginal Gyrus	L	−66, −23,31	5.19
	R	65, −31,35	3.51
Paracingulate Gyrus	R	11,37,22	5.18
Juxtapositional Lobule	R	11,3,53	5.14
Temporal Fusiform	R	34, −34, −27	5.12
Inferior Temporal Gyrus	R	61, −36, −17	5.03
Cingulate, Posterior	B	−2, −22,30	5.01
Central Opercular	R	41,11,5	5.01
Amygdala	R	14, −1, −15	4.94
Superior Parietal Lobule	L	−38, −56,52	4.88
	R	29, −42,41	4.87
	L	−26, −49,43	4.18
Cerebellar Lobule VI	L	−30, −34, −40	4.82
Parahippocampal Gyrus	L	−24,0, −38	4.66
	R	18, −7, −35	4.56
Brainstem	R	9, −27, −13	4.63
	B	0, −38, −12	4.44
	R	14, −23, −33	4.38
	B	−2, −32, −39	4.34
	R	7, −39, −38	4.28
Cingulate, Anterior	L	−8,17,30	4.59
	B	8, −6,34	4.31
Frontal Pole	R	−43,53,17	4.54
	L	−49,48, −7	4.50
	R	53,41,4	4.31
	L	−21,44, −18	4.29
	R	33,44, −16	4.18
	R	16,63, −18	4.08
	R	20,69, −6	4.03
Lateral Occipital	R	35, −68,25	4.54
	L	−20, −74,54	4.53
Middle Frontal Gyrus	L	−29, −4,58	4.46
Cerebellar VIIIa	R	37, −48, −51	4.37
Cerebellum (Dentate)	L	−22, −52, −39	4.29
Putamen	R	31, −6,9	4.28
Insula	L	−38,1,6	4.19
	L	−34,13,6	3.78
Thalamus (Pulvinar)	L	−19, −31,13	4.13
Middle Temporal Gyrus	R	54, −2, −35	3.92

* MNI = Montreal Neurological Institute standard space.

Table 3
SYMPT > ASYMPT Contrast.

Brain Region	Side	MNI*	Max Z-stat
Thalamus (Pulvinar)	B	10, −31,0	4.86
Inferior Frontal Gyrus	R	41,23,20	4.61
Occipital Fusiform Gyrus	R	38, −68, −17	4.34
Cerebellar Crus II	R	33, −81, −43	3.92
	R	33, −63, −45	3.64
	R	25, −75, −40	3.55
Frontal Orbital / Anterior Insula	L	−44,22, −9	3.87
Brainstem	L	−9, −36, −49	3.83

* MNI = Montreal Neurological Institute standard space.

inferior frontal gyrus, right occipital fusiform gyrus, right cerebellar crus II, left frontal orbital cortex, and left brainstem (Table 3). No areas showed significantly greater activation with ASYMPT visual stimulation.

The trigeminal nociceptive pathway was sparsely activated with both stimuli (Table 1), but no significant differences were detected between the two conditions. In this pathway, SYMPT only showed activation in bilateral ventroposteromedial thalamic nuclei, with no activation in the spinal trigeminal nuclei or trigeminal ganglia. ASYMPT showed activation in the brainstem near the vicinity of bilateral spinal trigeminal nuclei but no activation in ventroposteriomedial thalamic nuclei or trigeminal ganglia.

4. Discussion

In a patient with longstanding idiopathic photophobia, symptomatic vs. asymptomatic visual stimuli produced significantly greater activation in bilateral pulvinar nuclei. These thalamic nuclei are associated with the melanopsin ipRGC visual pathway (Allen et al., 2016; Maleki et al., 2012), and their activation is consistent with the patient's report that blue light differentially evoked photophobia. This appears to be the first demonstration of functional activation of the ipRGC pathway during photophobia in a patient.

4.1. Melanopsin

Several lines of evidence support the involvement of a melanopsin pathway with photophobia in this patient: (1) her report that cool blue light triggered her photophobia; (2) the fact that FL-41 tinted lenses, which filter melanopsin-related wavelengths of light, helped manage her photophobia; (3) the pulvinar nuclei, which have been previously structurally associated with the ipRGC pathway (Allen et al., 2016; Maleki et al., 2012), were significantly activated by the blue visual

stimuli that triggered photophobia; and (4) pulvinar nuclei activation has previously been related to migraine-related allodynia, which describes painful sensitivity to stimuli that is normally non-noxious (Burstein et al., 2010).

In healthy subjects without photophobia, melanopic signals have previously been shown to elicit fMRI responses in the bilateral frontal eye fields, inferior temporal gyri, caudate nuclei (Hung et al., 2017), as well as primary visual cortex (Spitschan et al., 2017). The lack of pulvinar activation in these healthy subjects in response to melanopic signals is consistent with our suggestion that this differential pulvinar activation represents a pathological process related to our patient's photophobia.

Considered together, these fMRI results suggest a sensitization of the ipRGC pathway beyond the retina. This hypothesis should be explored further in future studies that employ a larger patient cohort with greater statistical power, particularly when considering functional neuroimaging.

4.2. Trigeminal nociceptive pathway?

The photophobia responses observed in this patient are markedly different from our previous fMRI report of photophobia related to a corneal mechanism. Photophobia involving superficial corneal injury in a separate case study has previously been related to the trigeminal nociceptive pathway (Moulton et al., 2009; Moulton et al., 2012). Activation had been observed in the trigeminal ganglion ipsilateral to the injury, bilateral spinal trigeminal nuclei, contralateral ventroposteriomedial thalamus, and contralateral primary somatosensory cortex. After the photophobia had resolved, 9 days after the initial scan, these structures were no longer activated by the same visual stimulus protocol. In that study, photophobia was postulated to impact corneal sensory processing by sensitizing mechano-sensitive primary nociceptive afferents. Alternatively, recent findings that melanopsin is expressed in corneal afferents (Matynia et al., 2016) suggest that corneal injury may impact this non-image–forming light transduction pathway, thereby leading to photophobia. Conceivably, photophobia could result from activation of melanopsin-containing afferents in the cornea that cascade into the trigeminal nociceptive pathway.

Based on activation of the pulvinar nuclei in the present study, the melanopsin route in the patient appears to start with ipRGCs at the level of the retina. A direct path from the optic nerve at the level of the optic chiasm to the pulvinar nuclei has been demonstrated in humans using diffusion tensor imaging (Maleki et al., 2012). Though melanopsin is also expressed on afferents in the iris (Dolgonos et al., 2011; Xue et al., 2011) and cornea (Matynia et al., 2016), no activation of trigeminal nociceptive afferents was detected at the level of the trigeminal ganglion. Furthermore, no significant differences were detected between SYMPT and ASYMPT stimuli in any of the other structures in the trigeminal nociceptive pathway.

4.3. Beyond visual pathways

Several brain regions outside of traditional visual pathways were also found to be more active in the SYMPT vs. ASYMPT conditions. These may represent further downstream interpretive or reactive processes related to the stimulus induction of photophobia. For example, the anterior insula is related to affective pain processing (Apkarian et al., 2005; Price, 2000) and autonomic homeostasis, such as cardiovascular regulation (Oppenheimer and Cechetto, 2016). The posterior lobe of the cerebellum, including Crus II, is related to generalized aversive processing (Moulton et al., 2011) as well as the modulation of pain affect (Silva et al., 2019). In the prefrontal cortex, the inferior frontal gyrus is associated with cognitive reappraisal of painful experiences (Kelly et al., 2007). These regions and functions are consistent with the patient's report of photophobia.

4.4. Caveats

While our patient has been described as having longstanding idiopathic photophobia, several other factors may contribute to her symptoms, such as fibromyalgia. Clinical studies of fibromyalgia indicate that 70%–83% of patients exhibit photophobia (Heffez et al., 2004; Watson et al., 2009). Furthermore, fibromyalgia has a 55%–63% comorbidity with migraine (Marcus et al., 2005; Vij et al., 2015), which has photophobia as a defining characteristic. Though the patient reported no clinical diagnosis of migraine, a subclinical variant may have been present. Visual stimuli presented to chronic migraine patients has also been found to activate the trigeminal spinal nuclei (Schulte et al., 2018), although the description of the stimulus parameters lack detail. Other caveats relating to our specific study include the absence of controls for blurred vision, tachycardia, facial muscle contraction, nausea, and negative affect. Regardless of specific pathological etiology, this case report demonstrates activation of a known ipRGC thalamic relay in a patient with photophobia.

5. Conclusions

These findings and our previous photophobia case report (Moulton et al., 2009) support the theory that photophobia has at least two non-mutually exclusive pathways for its expression in patients: (1) through the ipRGC-optic nerve-pulvinar nuclei and (2) through the trigeminal nociceptive pathway by way of mechanical irritation and/or melanopsin stimulation of sensitized corneal afferents. While suggestive, these single-subject reports make a case for more systematic neuroimaging investigations to improve the diagnostic value of these findings. A larger cohort fMRI study with an appropriate control group would more definitively determine whether this ipRGC-pulvinar pathway is specific for this type of photophobia or whether the blue vs. red light paradigm preferentially activates this pathway in all subjects. The identification and classification of different mechanisms of photophobia may help with the diagnosis and treatment of underlying pathological conditions.

Funding

This work was supported by discretionary funds from the Center for Pain and the Brain (DB, EM), and the Department of Anesthesiology, Boston Children's Hospital (EM).

Author contributions

AP designed the stimulus delivery protocol, took part in data collection, interpreted the findings, and drafted the manuscript. DL and KS took part in data collection and assisted with drafting the manuscript. DB assisted with drafting the manuscript. EM conceptualized the experiment, took part in data collection, analyzed the data, interpreted the findings, and drafted the manuscript.

Declaration of Competing Interest

None.

Acknowledgements

We would like to acknowledge David P. Olson MD, PhD, Medical/Clinical Director of the McLean Imaging Center, who facilitated the logistical arrangements of scanning this patient at McLean Hospital, Scott Holmes PhD, from the Center for Pain and the Brain, for technical assistance with spatial registration.

References

Albilali, A., Dilli, E., 2018. Photophobia: when light hurts, a review. Curr Neurol Neurosci Rep 18, 62.

Allen, A.E., Procyk, C.A., Howarth, M., Walmsley, L., Brown, T.M., 2016. Visual input to the mouse lateral posterior and posterior thalamic nuclei: photoreceptive origins and retinotopic order. J Physiol 594, 1911–1929.

Apkarian, A.V., Bushnell, M.C., Treede, R.-.D., Zubieta, J.-.K., 2005. Human brain mechanisms of pain perception and regulation in health and disease. Eur J Pain 9, 463–484.

Avants, B.B., Tustison, N.J., Song, G., Cook, P.A., Klein, A., Gee, J.C., 2011. A reproducible evaluation of ANTs similarity metric performance in brain image registration. Neuroimage 54, 2033–2044.

Burstein, R., Jakubowski, M., Garcia-Nicas, E., Kainz, V., Bajwa, Z., Hargreaves, R., Becerra, L., Borsook, D., 2010. Thalamic sensitization transforms localized pain into widespread allodynia. Ann Neurol 68, 81–91.

Dolgonos, S., Ayyala, H., Evinger, C., 2011. Light-induced trigeminal sensitization without central visual pathways: another mechanism for photophobia. Invest Ophthalmol Vis Sci 52, 7852–7858.

Heffez, D.S., Ross, R.E., Shade-Zeldow, Y., Kostas, K., Shah, S., Gottschalk, R., Elias, D.A., Shepard, A., Leurgans, S.E., Moore, C.G., 2004. Clinical evidence for cervical myelopathy due to chiari malformation and spinal stenosis in a non-randomized group of patients with the diagnosis of fibromyalgia. Eur Spine J Off Publ Eur Spine Soc Eur Spinal Deform Soc Eur Sect Cerv Spine Res Soc 13, 516–523.

Hung, S.-M., Milea, D., Rukmini, A.V., Najjar, R.P., Tan, J.H., Viénot, F., Dubail, M., Tow, S.L.C., Aung, T., Gooley, J.J., Hsieh, P.-J., 2017. Cerebral neural correlates of differential melanopic photic stimulation in humans. Neuroimage 146, 763–769.

Jenkinson, M., Bannister, P., Brady, M., Smith, S., 2002. Improved optimization for the robust and accurate linear registration and motion correction of brain images. Neuroimage 17, 825–841.

Jenkinson, M., Smith, S., 2001. A global optimisation method for robust affine registration of brain images. Med Image Anal 5, 143–156.

Katz, B.J., Digre, K.B., 2016. Diagnosis, pathophysiology, and treatment of photophobia. Surv Ophthalmol 61, 466–477.

Kelly, S., Lloyd, D., Nurmikko, T., Roberts, N., 2007. Retrieving autobiographical memories of painful events activates the anterior cingulate cortex and inferior frontal gyrus. J Pain 8, 307–314.

Maleki, N., Becerra, L., Upadhyay, J., Burstein, R., Borsook, D., 2012. Direct optic nerve pulvinar connections defined by diffusion mr tractography in humans: implications for photophobia. Hum Brain Mapp 33, 75–88.

Marcus, D.A., Bernstein, C., Rudy, T.E., 2005. Fibromyalgia and headache: an epidemiological study supporting migraine as part of the fibromyalgia syndrome. Clin Rheumatol 24, 595–601.

Matynia, A., Nguyen, E., Sun, X., Blixt, F.W., Parikh, S., Kessler, J., Pérez de Sevilla Müller, L., Habib, S., Kim, P., Wang, Z.Z., Rodriguez, A., Charles, A., Nusinowitz, S., Edvinsson, L., Barnes, S., Brecha, N.C., Gorin, M.B., 2016. Peripheral sensory neurons expressing melanopsin respond to light. Front Neural Circuits 10, 60.

Moulton, E., Becerra, L., Borsook, D., 2009. An fMRI case report of photophobia: activation of the trigeminal nociceptive pathway. Pain 145, 358–363.

Moulton, E.A., Becerra, L., Rosenthal, P., Borsook, D., 2012. An approach to localizing corneal pain representation in human primary somatosensory cortex. PLoS ONE 7, e44643.

Moulton, E.A., Elman, I., Pendse, G., Schmahmann, J., Becerra, L., Borsook, D., 2011. Aversion-related circuitry in the cerebellum: responses to noxious heat and unpleasant images. J Neurosci 31, 3795–3804.

Noseda, R., Copenhagen, D., Burstein, R., 2018. Current understanding of photophobia, visual networks and headaches. Cephalalgia Int J Headache 333102418784750.

Noseda, R., Kainz, V., Jakubowski, M., Gooley, J.J., Saper, C.B., Digre, K., Burstein, R., 2010. A neural mechanism for exacerbation of headache by light. Nat Neurosci 13, 239–245.

Okamoto, K., Tashiro, A., Chang, Z., Bereiter, D.A., 2010. Bright light activates a trigeminal nociceptive pathway. Pain 149, 235–242.

Oppenheimer, S., Cechetto, D., 2016. The insular cortex and the regulation of cardiac function. Comprehensive Physiology. American Cancer Society 1081–1133. https://doi.org/10.1002/cphy.c140076.

Price, D.D., 2000. Psychological and neural mechanisms of the affective dimension of pain. Science 288, 1769–1772.

Rosenthal, P., Borsook, D., 2012. The corneal pain system. part I: the missing piece of the dry eye puzzle. Ocul Surf 10, 2–14.

Schulte, L.H., Allers, A., May, A., 2018. Visual stimulation leads to activation of the nociceptive trigeminal nucleus in chronic migraine. Neurology 90, e1973–e1978.

Silva, K.E., Rosner, J., Ullrich, N.J., Chordas, C., Manley, P.E., Moulton, E.A., 2019. Pain affect disrupted in children with posterior cerebellar tumor resection. Ann Clin Transl Neurol 6, 344–354.

Smith, S.M., 2002. Fast robust automated brain extraction. Hum Brain Mapp 17, 143–155.

Smith, S.M., Jenkinson, M., Woolrich, M.W., Beckmann, C.F., Behrens, T.E.J., Johansen-Berg, H., Bannister, P.R., De Luca, M., Drobnjak, I., Flitney, D.E., Niazy, R.K., Saunders, J., Vickers, J., Zhang, Y., De Stefano, N., Brady, J.M., Matthews, P.M., 2004. Advances in functional and structural mr image analysis and implementation as fsl. Neuroimage 23 (Suppl 1), S208–S219.

Spitschan, M., Bock, A.S., Ryan, J., Frazzetta, G., Brainard, D.H., Aguirre, G.K., 2017. The human visual cortex response to melanopsin-directed stimulation is accompanied by a distinct perceptual experience. Proc Natl Acad Sci 114, 12291–12296.

Vij, B., Whipple, M.O., Tepper, S.J., Mohabbat, A.B., Stillman, M., Vincent, A., 2015. Frequency of migraine headaches in patients with fibromyalgia. Headache 55, 860–865.

Watson, N.F., Buchwald, D., Goldberg, J., Noonan, C., Ellenbogen, R.G., 2009. Neurologic signs and symptoms in fibromyalgia. Arthritis Rheum 60, 2839–2844.

Woolrich, M.W., Ripley, B.D., Brady, M., Smith, S.M., 2001. Temporal autocorrelation in univariate linear modeling of fmri data. Neuroimage 14, 1370–1386.

Worsley, K.J., 2001. Statistical analysis of activation images. In: Jezzard, P., Matthews, PM, Smith, SM (Eds.), Functional MRI: An Introduction to Methods. Oxford University Press, pp. 251–270.

Xue, T., Do, M.T.H., Riccio, A., Jiang, Z., Hsieh, J., Wang, H.C., Merbs, S.L., Welsbie, D.S., Yoshioka, T., Weissgerber, P., Stolz, S., Flockerzi, V., Freichel, M., Simon, M.I., Clapham, D.E., Yau, K.-W., 2011. Melanopsin signalling in mammalian iris and retina. Nature 479, 67–73.